# Syntheses, Structures and Photophysical Properties of Metal Carbonyl Clusters with Dansyl and Acridone Luminophores

**Wai-Yeung Wong,*[a] Ka-Ho Choi,[a] and Zhenyang Lin[b]**

**Keywords:** Transition metal / Dansyl group / Acridone / Luminophores

A series of fluorescent transition metal complexes bearing the 5-(dimethylamino)naphthalene-1-sulfonyl ($R^1$) and acridone ($R^2$) frameworks have been prepared. Reactions of the fluorescent-labeled alkyne ligands $R^1CH_2C{\equiv}CH$ and $R^2CH_2C{\equiv}CH$ with various metal carbonyl compounds $[Co_2(CO)_8]$, $[Et_3NH][Fe_2(CO)_6(\mu\text{-}CO)(\mu\text{-}S\textit{t}Bu)]$ and $[M_3(CO)_{10}(NCMe)_2]$ (M = Ru, Os) readily afforded new cluster complexes of the stoichiometry $[Co_2(CO)_6(\mu\text{-}\eta^2\text{-}RCH_2CCH)]$ (**1**: R = $R^1$, **2**: $R^2$), $[Fe_2(CO)_6(\mu\text{-}S\textit{t}Bu)(\mu\text{-}\eta^2\text{-}RCH_2C{=}CH_2)]$ (**3**: R = $R^1$, **4**: $R^2$), $[Ru_3(CO)_9(\mu\text{-}CO)(\mu_3\text{-}\eta^2\text{-}RCH_2CCH)]$ (**5**: R = $R^1$, **6**: $R^2$) and $[Os_3(CO)_9(\mu\text{-}CO)(\mu_3\text{-}\eta^2\text{-}RCH_2CCH)]$ (**7**: R = $R^1$, **8**: $R^2$) in moderate to good yields. All of these new complexes have been fully characterized by FTIR, $^1H$ NMR spectroscopy, UV/Vis spectroscopy and fast atom bombardment mass spectrometry (FABMS). The single-crystal X-ray structural analyses and molecular orbital calculations on **1**, **2**, **4** and **8** have been performed. It was found that all of these compounds are fluorescent in solutions at room temperature and a luminescence band characteristic of the inherent fluorophore is observed in these metal structures. However, a strong quenching of the fluorescence intensity of the chromophoric groups was observed upon coordination of metal cluster moieties.



## Introduction

Photoluminescence spectroscopy has continued to attract increasing current attention in the scientific community due to its wide applications in environmental and biological sciences and molecular electronics.[1−6] The preparation and photophysical properties of several fluorescent methylmercury acetylides carrying the anthracene, 5-(dimethylamino)naphthalene-1-sulfonyl (dansyl) and 9-acridone frameworks have recently been reported and these compounds could be exploited in the development of new analytical methods for methylmercury in environmental and biological samples.[7] Prodi and co-workers also described the use of a tripodal ligand containing the dansyl chromophore as a luminescent chemosensor for metal ions.[8]

We have a long-term interest in the design and synthesis of luminescent transition metal-containing materials[9,10] and major efforts have been devoted to the studies of organometallic acetylide complexes and polymers incorporating a vast range of aromatic and heteroaromatic spacers.[11−16] In view of the high luminescence quantum yields of the auxiliary dansyl and acridone units,[17] we expect that a properly derivatized molecule such as 5-(dimethylamino)-*N*-(2-propynyl)-1-naphthalenesulfonamide (**I**) and 10-(2-propynyl)-9-acridone (**II**) (Scheme 1) could be employed to attach a fluorescent label to the metal center through an acetylide linkage,[7,10] which is likely to exhibit rich optical and photo-electronic properties. Indeed, two novel blue luminescent platinum(II) acetylide compounds bearing these functionalities have been reported recently by us in preliminary form.[10] We therefore sought to design new molecular systems featuring these luminophores. In this context, we aim at preparing some fluorescent-labeled metal carbonyl complexes of Groups 8 and 9 transition metal elements by using properly tailored acetylenes since the interactions between alkynes and binary low-nuclearity carbonyl complexes of iron, ruthenium, osmium and cobalt have been well documented.[18−28] To the best of our knowledge, studies of luminescent transition metal carbonyl clusters bearing fluorescent labels are scarce. In this article, we describe the synthesis, as well as the spectroscopic, structural and photophysical properties of a new series of fluorescent dinuclear and trinuclear metal complexes incorporating the dansyl and acridone entities.

## Results and Discussion

### Synthesis

An adaptation of the literature methods was employed to obtain the fluorescent-labeled ligands **I** and **II**.[7,10] The synthetic routes to all the new compounds are shown in Scheme 2. The dinuclear cobalt carbonyl complexes **1** and

[a] Department of Chemistry, Hong Kong Baptist University, Waterloo Road, Kowloon Tong, Hong Kong, P. R. China
E-mail: rwywong@hkbu.edu.hk
[b] Department of Chemistry, The Hong Kong University of Science and Technology, Clearwater Bay, Hong Kong, P. R. China

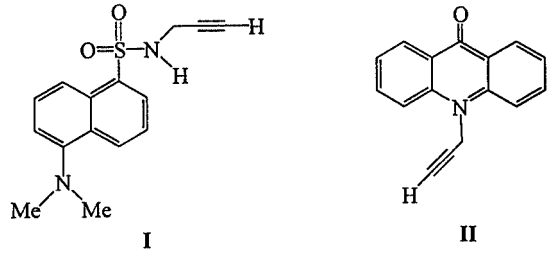

Scheme 1. Structures of **I** and **II**

**2** were prepared in moderate yields by reacting $[Co_2(CO)_8]$ with one equivalent of **I** and **II**, respectively, at 0 °C.[25−28] Thermal treatment of **I** and **II** with the iron carbonyl salt $[Et_3NH][Fe_2(CO)_6(\mu\text{-}CO)(\mu\text{-}S\textit{t}Bu)]$ prepared in situ from a $[Fe_3(CO)_{12}]/NEt_3/\textit{t}BuSH$ mixture[18] in a 1:1 molar ratio in refluxing THF afforded the σ,π-vinyl complexes **3** and **4** in yields of 31 and 35%, respectively. This reaction sequence was accompanied by the formation of $[Fe_2(CO)_6(\mu\text{-}S\textit{t}Bu)_2]$ as a by-product.[18] The reactions of the freshly prepared $[Ru_3(CO)_{10}(NCMe)_2]$ with the appropriate alkynes **I** and **II** are straightforward at room temperature with the loss of MeCN to give complexes **5** and **6** as the final products. The facile displacement of two MeCN groups of $[Os_3(CO)_{10}(NCMe)_2]$ by the terminal acetylenes to afford $[Os_3(CO)_9(\mu\text{-}CO)(\mu_3\text{-}\eta^2\text{-}RCCH)]$ was successfully applied to the preparation of alkyne-substituted complexes **7** and **8** as major products.[21−23] All of these compounds were purified by preparative TLC on silica and compounds **1**−**4** were isolated as orange to red solids and products **5**−**8** as yellow solids. Complexes **1**−**8** are highly soluble in common organic solvents such as $CH_2Cl_2$ and $CHCl_3$ and their solutions slowly decompose when exposed to air. As solid materials they are stable at room temperature for prolonged periods even when precautions to exclude air or moisture are not taken.

### Spectroscopic Properties

Collated spectroscopic data (IR, $^1H$ NMR and FABMS) of these new fluorophore-anchored metal complexes are in agreement with their formulation and full details are given in the Exp. Sect. The disappearance of the IR ν(C≡C) and ν(≡C−H) bands in **1**−**8** indicates that metal carbonyl fragments are coordinated to the acetylenic unit. A broad peak at 1880 $cm^{-1}$ for the Ru complexes **5** and **6**, and 1848 $cm^{-1}$ for the osmium derivatives **7** and **8**, was consistent with the presence of a bridging carbonyl group in each case. In the IR spectra, the band patterns between the uncomplexed and complexed chromophores are similar. Coordination of the alkyne moiety to the metal core was confirmed by the close resemblance of the IR spectral pattern in the ν(CO) region of our complexes with those observed for the reported cobalt−alkyne complexes,[25−28] $[Fe_2(CO)_6(\mu\text{-}SR)(\mu\text{-}\eta^2\text{-}R'C{=}CH_2)]$[18,29] and $'M_3(CO)_{10}'$ cores (M = Ru, Os) which coordinate an alkyne in a $\mu_3\text{-}(\eta^2\text{-}\|)$ fashion.[21−24] The $^1H$ NMR spectra of the new complexes display resonances stemming from the coordinated dansyl or acridone group but the signals due to −C≡CH for **I** (ca. 1.92 ppm) and **II** (ca. 2.43 ppm) were absent.[7] Except for **3** and **4**, the presence of a singlet peak in the range of δ = 5.74−9.10 is clearly resolved for the −CCH protons in these compounds. Assignments for the signals arising from the protons attached to $C_\beta$ in the vinyl-bridged diiron compounds **3** and **4** could be made in their corresponding $^1H$ NMR spectra

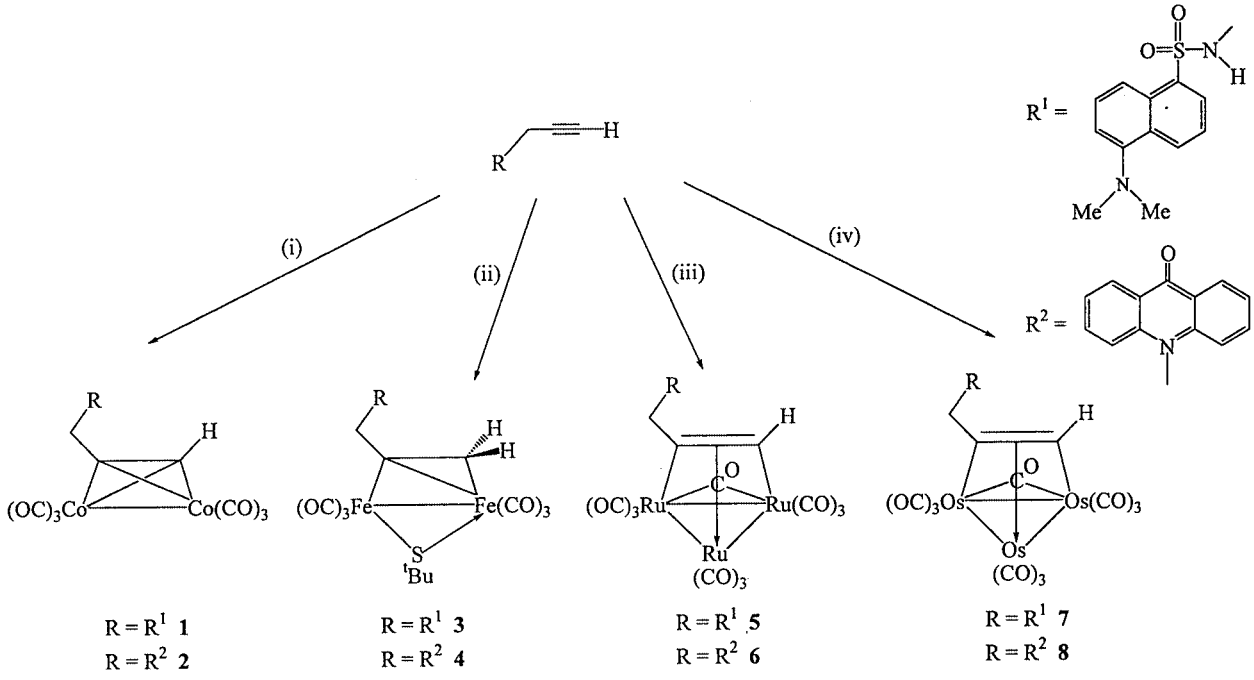


Scheme 2. (i) $[Co_2(CO)_8]$, hexane, 1 h, 0 °C; (ii) $[Et_3NH][Fe_2(CO)_6(\mu\text{-}CO)(\mu\text{-}S\textit{t}Bu)]$, THF, reflux, 5 h; (iii) $[Ru_3(CO)_{10}(NCMe)_2]$, $CH_2Cl_2$/MeCN, room temp., 2 h; (iv) $[Os_3(CO)_{10}(NCMe)_2]$, $CH_2Cl_2$, room temp., 2 h.

consistent for both structures. For **3**, the two vinyl proton resonances appear as two doublets at δ = 2.63 and 3.48 ppm with a geminal coupling constant of 2.6 Hz, whereas two doublets are apparent at δ = 2.77 and 3.13 ppm ($J_{H-H}$ = 4.6 Hz) for **4**. These data agree with those reported for other [$Fe_2(CO)_6$(μ-SR)(μ-R′$C_α$=$C_βH_2$)] complexes and they are consistent with NMR spectroscopic data for other μ-vinyl systems as well.[18,29] The thiolate moieties in **3** and **4** display the expected singlet peak due to the *tert*-butyl group. These new compounds also gave satisfactory mass spectroscopic data and, in most cases, they showed the molecular ion peaks followed by the consecutive loss of carbonyl fragments. The parent ion peaks indicate a 1:1 (metal/ligand) stoichiometry for the complexes.

### Electronic Absorption and Luminescence Spectra

The photophysical properties of complexes **1**−**8** have been studied in $CH_2Cl_2$ at room temperature and the results are summarized in Table 1. Both of the free alkynes **I** and **II** typically exhibit three intense absorption peaks in the near-UV region that can be ascribed to π−π* transitions within the ligand framework.[10] For the metal cluster complexes, they all show similar structured low-energy bands in the near-UV and the visible regions due to the metal-perturbed intraligand π−π* transitions of the organic units. At the lowest energy regime, absorptions probably arise from the ligand-to-cluster core charge transfer transitions for each appropriate metal cluster fragment (vide infra). Excitation of **1**−**8** in $CH_2Cl_2$ solutions results in a blue to greenish-blue luminescence band peaking in the range of 506−509 nm for the dansyl derivatives and of 425−431 nm for the acridone counterparts (Figure 1 and Figure 2). The emission wavelengths of the dansyl complexes remain relatively unshifted with respect to that of **I** but we observe a slight bathochromic shift in the peak maxima for the acridone congeners as compared to that of **II**. These featureless luminescence spectra are independent of the excitation wavelength used. Due to their similar structured peak pattern, we consider that the emission features between the uncomplexed and complexed fluorophores should have the same origin for each case and are most likely caused by the metal-perturbed dansyl or acridone emission. Of particular relevance here is the observation of a strong quenching of the fluorescence intensity of the luminophores upon metal coordination in all the cases studied. The fluorescence quantum yields of the metal complexes are less than those of **I** and **II** by one to two orders of magnitude. With reference to previous work on other organometallic systems, we can attribute the quenching in the luminescence intensity to the so-called heavy-atom effect, an energy-transfer or an electron-transfer mechanism.[7,8]

### Crystal Structure Analyses

The single-crystal X-ray structures of **1**, **2**, **4** and **8** were established unambiguously and the perspective views are depicted in Figures 3−6, respectively. Pertinent bond

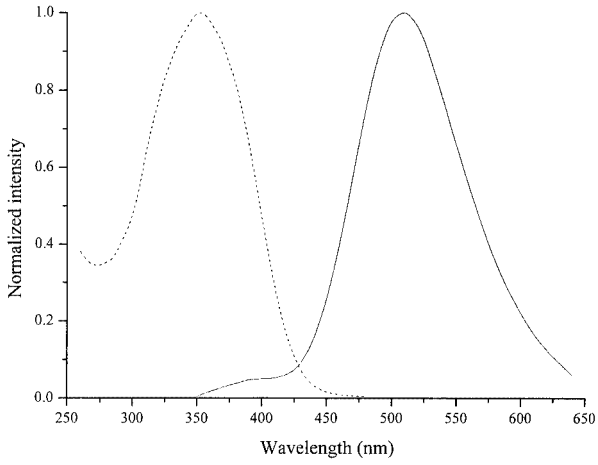


Figure 1. Excitation (---) and photoluminescence (—) spectra of **1** in $CH_2Cl_2$ at room temperature

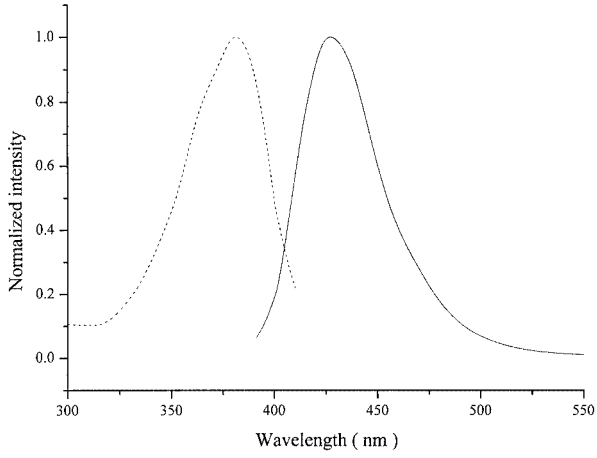


Figure 2. Excitation (---) and photoluminescence (—) spectra of **2** in $CH_2Cl_2$ at room temperature

lengths and angles are collected in Tables 2−5. Structurally, the essential features of both **1** and **2** are very similar in which the Co(1)−Co(2) axis forms a pseudo-tetrahedron with the C≡C bond of the alkynyl ligands **I** and **II** with the C≡C vector lying perpendicular to the Co−Co vector. In each case, the Co−Co separation [2.492(1) **1**, 2.4791(4) Å **2**] is in the region expected for other $Co_2$-alkyne systems.[25−28] The C(7)−C(8) bond lengths for **1** and **2** are 1.341(7) and 1.333(3) Å, respectively, suggestive of the loss of the triple bond character of the alkyne ligands upon complexation. There are no unusual structural parameters in the chromophoric groups of both molecules.

The basic structure of **4** consists of a diiron hexacarbonyl core in which the Fe−Fe edge [2.534(2) Å] is bridged by the thiolate and μ-σ-vinyl groups. The thiolate bridge itself spans the Fe−Fe bond asymmetrically with the Fe(1)−S(1) and Fe(2)−S(1) distances being 2.239(2) and 2.279(3) Å, respectively. While the iron−sulfur distances are typical of thiolate-bridged diiron compounds,[29−31] the C(7)−S(1) bond of 1.848(9) Å is slightly longer than the normal carbon−sulfur single bonds of 1.815(1) Å,[32] and this indic-

Table 1. Electronic absorption and emission data for complexes **1**−**8**

| Compound | $\lambda_{max}$/nm ($\varepsilon \times 10^{-4}$/M$^{-1}$ cm$^{-1}$)[a] | $\lambda_{em}$/nm ($10^3 \times \Phi$)[a] |
|---|---|---|
| **I**[7] | 230 (1.4), 253 (1.6), 345 (0.5) | 508 (450) |
| **II**[7] | 250 (3.6), 373 (1.9), 390 (2.4) | 417 (8.0) |
| **1** | 253 (2.9), 312 (0.8), 348 (0.9) | 509 (5.0) |
| **2** | 248 (3.7), 304 (0.7), 358 (0.8), 378 (1.0), 396 (1.3) | 427 (0.1) |
| **3** | 232 (1.8), 252 (1.8), 336 (0.6), 469 (0.1) | 506 (7.5) |
| **4** | 250 (2.3), 375 (1.1), 395 (1.4), 460 (0.2) | 404, 425 (3.2) |
| **5** | 230 (2.3), 250 (2.1), 340 sh (0.6), 477 sh (0.1) | 506 (1.4) |
| **6** | 230 sh (2.8), 254 (3.8), 381 (0.8), 397 (1.0), 468 sh (0.1) | 429 (0.6) |
| **7** | 248 (0.3), 342 sh (0.1), 440 sh (0.02) | 506 (4.3) |
| **8** | 232 sh (1.5), 254 (2.3), 380 (1.1), 398 (1.6), 442 sh (0.2) | 431 (0.4) |

[a] In $CH_2Cl_2$. sh = shoulder

ates some delocalization of electron density from the thiolate bridge into the metal core. The C(11)−C(12) bond is bound to Fe(2) via a π-interaction [Fe(2)−C(11) 2.131(7), Fe(2)−C(12) 2.14(1) Å] and to Fe(1) via a σ bond [Fe(1)−C(11) 1.983(8) Å]. The C(11)−C(12) bond length of 1.37(1) Å is characteristic of this type of vinylic coordination. The six carbonyl ligands are all terminally bound and essentially linear. By regarding both the vinyl and μ-SR groups as three-electron donors, complex **4** has 34 cluster valence electrons and is electron precise.

For **8**, the triosmium unit is coordinated to an alkyne moiety in a classical $\mu_3$-($\eta^2$-||) manner via two σ bonds through Os(1) and Os(3) and a typical π bond to Os(2). This creates the nido-octahedral $M_3C_2$ core geometry expected for this type of coordination. The alkyne-metal σ bonds are 2.135(7) and 2.085(6) Å long, while the relevant π-interactions are characteristically longer at 2.181(6) and 2.315(6) Å. The C(11)−C(12) edge bridges the Os(1)−Os(3) bond to afford a four-membered metallacyclic ring, which makes a dihedral angle of 58.1° with the $Os_3$ triangle. The observation that the C(3)−Os(1)−Os(3) and Os(1)−C(3)−O(3) bond angles of 64.7(2) and 163.3(7)°, respectively, suggests that this carbonyl ligand is tending towards a semi-bridging interaction. In **2**, **4** and **8**, the acridone ring is almost planar (mean deviation is ca. 0.016−0.047 Å) and no evidence of intermolecular stacking interaction between individual acridone units in the crystal lattice was observed in each case.

## Molecular Orbital Calculations

In order to study the electronic structures for the new clusters, we have performed molecular orbital calculations on **1**, **2**, **4** and **8** at the B3LYP level of density functional theory (DFT) based on their experimental geometries from X-ray data (see Computational Details section). The characteristics of the molecular orbitals in the frontier region are comparable for these four complexes. The contour plots[33] of the highest occupied (HOMO) and lowest unoccupied (LUMO) molecular orbitals for **1** and **2** are shown in Figure 7. The DFT calculations show that the HOMO−LUMO gaps for the four clusters are close to each other (ca. 23,356 **1**, 23,354 **2**, 25,119 **4** and 23,920 cm$^{-1}$ **8**).

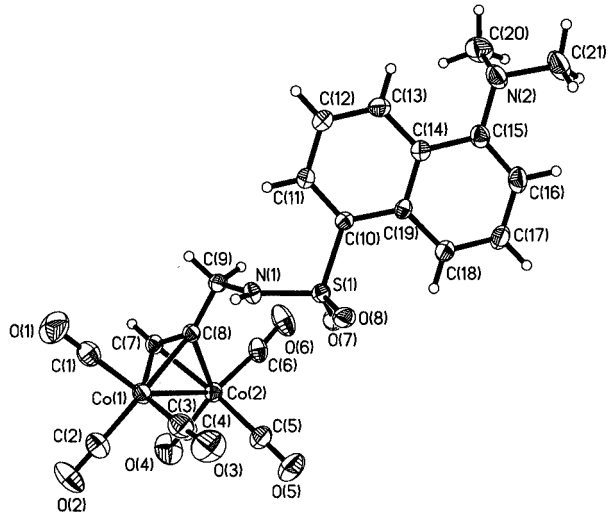


Figure 3. A perspective drawing of compound **1** with the atoms shown at the 25% probability level

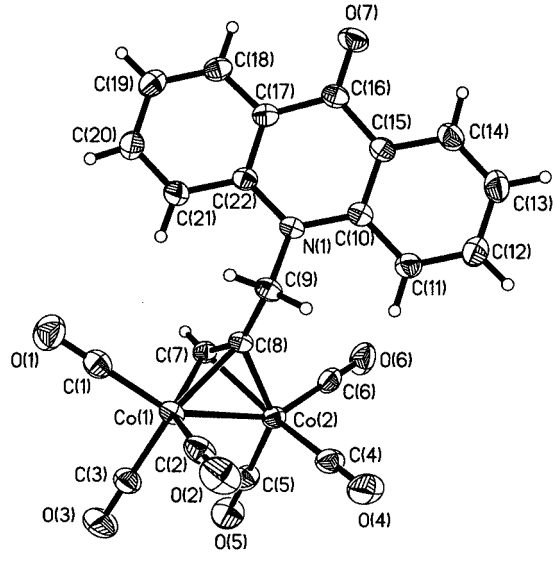


Figure 4. A perspective drawing of compound **2** with the atoms shown at the 25% probability level

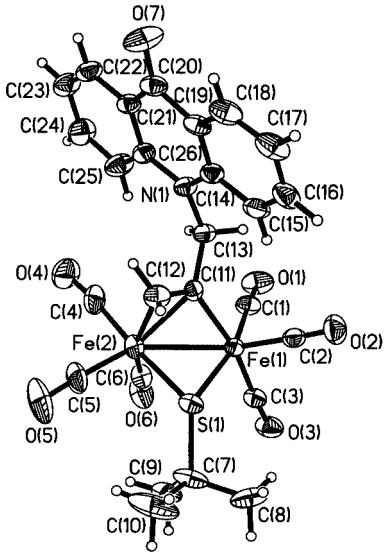


Figure 5. A perspective drawing of compound **4** with the atoms shown at the 25% probability level

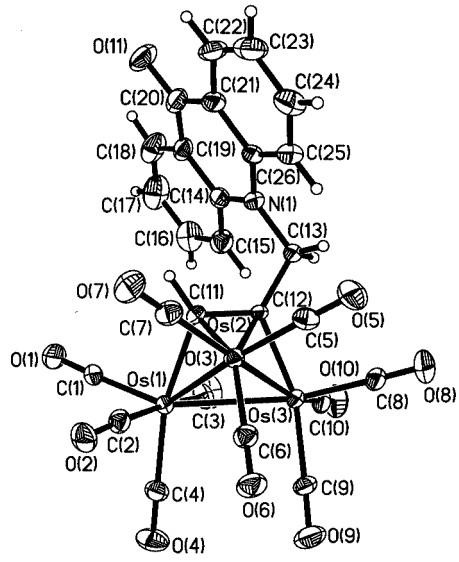


Figure 6. A perspective drawing of compound **8** with the atoms shown at the 25% probability level

Table 2. Selected bond lengths (Å) and angles (°) for complex **1**

| | | | |
|---|---|---|---|
| Co(1)−Co(2) | 2.492(1) | Co(1)−C(7) | 1.969(6) |
| Co(1)−C(8) | 1.953(5) | Co(2)−C(7) | 1.934(6) |
| Co(2)−C(8) | 1.962(6) | C(7)−C(8) | 1.341(7) |
| N(1)−S(1) | 1.614(5) | S(1)−O(7) | 1.431(4) |
| S(1)−O(8) | 1.444(4) | | |
| Co(2)−Co(1)−C(7) | 49.7(2) | Co(2)−Co(1)−C(8) | 50.6(2) |
| Co(1)−Co(2)−C(7) | 50.9(2) | Co(1)−Co(2)−C(8) | 50.3(2) |
| C(7)−C(8)−C(9) | 138.2(5) | | |

The common feature of the HOMOs and LUMOs of these metal clusters is that the HOMO corresponds to the π bonding in the aromatic unit of the bridging acetylene ligand and the LUMO involves metal−metal antibonding,

Table 3. Selected bond lengths (Å) and angles (°) for complex **2**

| | | | |
|---|---|---|---|
| Co(1)−Co(2) | 2.4791(4) | Co(1)−C(7) | 1.974(2) |
| Co(1)−C(8) | 1.970(2) | Co(2)−C(7) | 1.972(2) |
| Co(2)−C(8) | 1.972(2) | C(7)−C(8) | 1.333(3) |
| Co(2)−Co(1)−C(7) | 51.03(5) | Co(2)−Co(1)−C(8) | 51.06(5) |
| Co(1)−Co(2)−C(7) | 51.11(5) | Co(1)−Co(2)−C(8) | 51.00(5) |
| C(7)−C(8)−C(9) | 144.8(2) | | |

Table 4. Selected bond lengths (Å) and angles (°) for complex **4**

| | | | |
|---|---|---|---|
| Fe(1)−Fe(2) | 2.534(2) | Fe(1)−C(11) | 1.983(8) |
| Fe(1)−S(1) | 2.239(2) | Fe(2)−C(11) | 2.131(7) |
| Fe(2)−C(12) | 2.14(1) | Fe(2)−S(1) | 2.279(3) |
| C(11)−C(12) | 1.37(1) | S(1)−C(7) | 1.848(9) |
| Fe(1)−Fe(2)−C(11) | 49.4(2) | Fe(1)−Fe(2)−C(12) | 79.5(3) |
| Fe(1)−C(11)−Fe(2) | 75.9(3) | Fe(1)−S(1)−Fe(2) | 68.23(8) |
| Fe(2)−Fe(1)−C(11) | 54.7(2) | Fe(2)−C(11)−C(12) | 71.8(6) |
| C(11)−Fe(2)−C(12) | 37.3(4) | C(12)−C(11)−C(13) | 116.5(8) |
| Fe(1)−Fe(2)−S(1) | 55.14(7) | Fe(2)−Fe(1)−S(1) | 56.63(7) |

Table 5. Selected bond lengths (Å) and angles (°) for complex **8**

| | | | |
|---|---|---|---|
| Os(1)−Os(2) | 2.8276(4) | Os(1)−Os(3) | 2.8983(4) |
| Os(2)−Os(3) | 2.7194(4) | Os(1)−C(11) | 2.135(7) |
| Os(2)−C(11) | 2.181(6) | Os(2)−C(12) | 2.315(6) |
| Os(3)−C(12) | 2.085(6) | C(11)−C(12) | 1.418(8) |
| Os(1)−Os(2)−Os(3) | 62.966(9) | Os(1)−Os(3)−Os(2) | 60.342(9) |
| Os(1)−C(11)−C(12) | 108.8(4) | Os(2)−C(11)−C(12) | 76.8(4) |
| Os(3)−C(12)−C(11) | 111.3(4) | C(11)−Os(2)−C(12) | 36.6(2) |
| C(11)−C(12)−C(13) | 122.4(5) | | |

suggesting a dominant ligand-to-metal charge transfer character of their lowest HOMO−LUMO electronic transition. In the related work, the HOMO for **I** was found to possess a significant contribution from the pπ orbital of the $NMe_2$ group in addition to the π bonding feature within the aromatic unit, whereas the LUMO corresponds to the π* orbital of the aromatic moiety. The energy gap was calculated to be 33,792 $cm^{-1}$, which is much greater than that of **1**. Contrary to what we have observed here, previous calculations on other $[Os_3(CO)_{10}(\alpha\text{-diimine})]$ clusters[34,35] showed that the HOMOs are mainly metal orbital-based (Os−Os bonding) while the LUMOs are more localized on the α-diimine ligand. Clearly, the bridging acetylene ligands in the currently studied clusters, significantly affect the orbital structures in the HOMO−LUMO region. Examining the orbital energies in the HOMO−LUMO region for our compounds, we found that the molecular orbitals derived from metal d-orbitals (both bonding and antibonding) are shifted down to a lower energy region and the π and π* orbitals of the aromatic units in the ligands go up in energy in comparison to the corresponding MOs calculated for the $[Os_3(CO)_{10}(diimine)]$-type clusters mentioned above. It is because of these changes in the orbital energies that we observe the totally different patterns between the alkyne- and

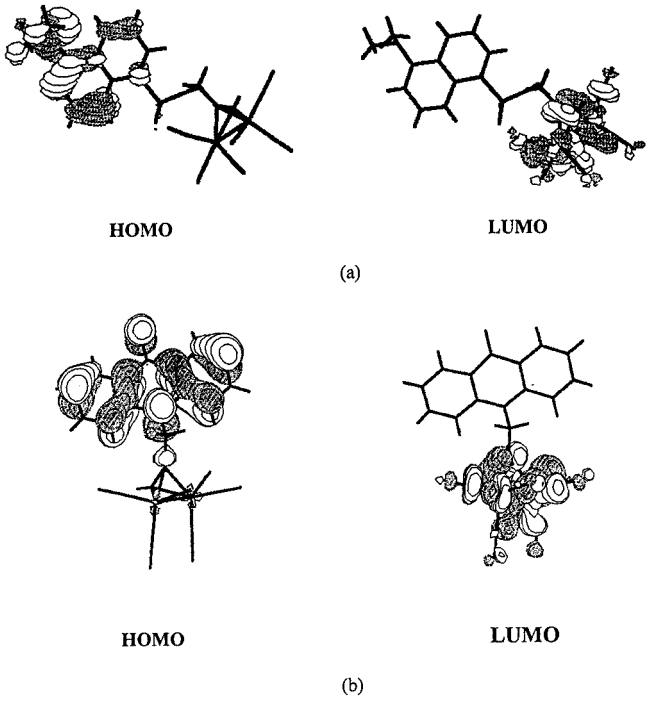


Figure 7. Spatial plots of the highest occupied (HOMO) and the lowest unoccupied molecular orbitals (LUMO) for complexes (a) **1** and (b) **2**

diimine-bridged compounds. The stabilization of the metal d-orbital-based MOs can be related to the π*-accepting properties and strong binding abilities of the bridging acetylene ligands. Since the LUMOs for these clusters involve metal−metal antibonding, and by considering the possible fragmentation, we expect that the life-time of an excited state of such clusters is much shorter when compared to other types of clusters in which there is a significant contribution of the ligands to the LUMOs. This probably results in a poor fluorescence quantum efficiency of the clusters in the present study.

## Concluding Remarks

Our present work provides a simple access to a new family of alkyne-derived fluorescent-labeled metal clusters. A series of metal complexes of Groups 8 and 9 elements containing dansyl and acridone chromophores have been synthesized in moderate yields and spectroscopically and photophysically characterized. These new compounds are shown to be emissive in the blue to green-blue region in solutions at room temperature and quenched luminescence bands typical of the fluorophores are observed. In this work, we have also demonstrated how one can modulate the luminescence properties of the fluorophore in the presence of a variety of metal cluster cores and such a quenching process is particularly crucial to our understanding in the development of new molecular luminescent sensing systems. The effect of other transition metals on the luminescent behavior and a more in-depth investigation on analytical applications of these systems will be the subject of a future study.

## Experimental Section

General Procedures: All reactions were conducted under an atmosphere of dry nitrogen with the use of standard Schlenk techniques. Solvents for preparative work were dried and distilled before use. Unless otherwise stated all reagents were obtained from commercial suppliers and used without further purification. The syntheses of ligand precursors **I** and **II**[7] and the complexes $[Et_3NH][Fe_2(CO)_6(\mu\text{-}CO)(\mu\text{-}S\textit{t}Bu)]$[18] and $[M_3(CO)_{10}(NCMe)_2]$ (M = Ru, Os)[36,37] were carried out as reported previously. IR spectra were recorded as $CH_2Cl_2$ solutions on a Perkin−Elmer Paragon 1000 PC or Nicolet Magna 550 Series II FTIR spectrometer. Proton NMR spectra were measured in $CDCl_3$ on a JEOL EX270 or a Varian Inova 400 MHz FT NMR spectrometer, with chemical shifts quoted relative to $SiMe_4$. Fast atom bombardment (FAB) mass spectra were recorded in *m*-nitrobenzyl alcohol matrices on a Finnigan-SSQ 710 spectrometer. Electronic absorption spectra were obtained with an HP 8453 or Cary 100 UV/Vis spectrometer. Corrected emission and excitation spectra were obtained in $CH_2Cl_2$ with a Perkin−Elmer LS50B or PTI QM1 spectrofluorimeter. The fluorescence quantum yields were determined in $CH_2Cl_2$ solutions at 290 K against the anthracene standard in the same solvent ($\Phi$ = 0.27).[38] Separation of products was accomplished by preparative TLC plates coated with silica (Merck, Kieselgel 60).

Computational Details: Density functional theory calculations at the B3LYP level[39−41] were performed on **1**, **2**, **4** and **8** based on their experimental geometries from X-ray crystallographic data. The basis set used for C, H N and O atoms was 6−31G[42] while effective core potentials with a LanL2DZ basis set[43] were employed for Co, Fe and Os atoms. All calculations were performed with the use of Gaussian 98.[44] In view of the large systems studied here and computing resources available to us, we did not use basis sets with higher quality. Addition of polarization functions to C, N and O would increase the number of basis functions by more than a hundred. Previous molecular orbital calculations on other related systems[45,46] showed that the medium-size basis set provides reasonable results. In addition, we are interested in obtaining the qualitative picture of orbital patterns for the clusters and in comparing the relative HOMO−LUMO gaps. We believe that the addition of polarization functions in our calculations will not alter the conclusions we have made.

**$[Co_2(CO)_6(\mu\text{-}\eta^2\text{-}R^1CH_2CCH)]$ (1):** $[Co_2(CO)_8]$ (32.1 mg, 0.09 mmol) was dissolved in degassed hexane (10 mL) and the solution was stirred at 0 °C under $N_2$. The alkyne ligand **I** (22.9 mg, 0.10 mmol) in $CH_2Cl_2$ (3 mL) was subsequently added. After the mixture was stirred for 1 h, the solvent was removed under reduced pressure. The residue was purified by preparative TLC on silica using hexane/$CH_2Cl_2$ (1:1, v/v) as eluent to furnish a major brown-red band. The title product was recrystallized from hexane−$CH_2Cl_2$ to give deep red crystals of **1** in 32% yield (17.3 mg). IR ($CH_2Cl_2$): ν(N−H) = 3384 w, ν(CO) = 2097s, 2058 vs and 2031 vs $cm^{-1}$. $^1H$ NMR ($CDCl_3$): δ = 2.88 (s, 6 H, $NMe_2$), 4.20 (s, 2 H, $NCH_2$), 4.91 (s, 1 H, NH), 5.74 (s, 1 H, CCH), 7.21 (m, 1 H, aromatic), 7.55 (t, $J_{H-H}$ = 7.6 Hz, 2 H, aromatic), 8.30 (m, 2 H, aromatic) and 8.55 (d, $J_{H-H}$ = 8.6 Hz, 1 H, aromatic). FAB MS: *m*/*z* = 490 [(M − 3CO)$^+$]. $C_{21}H_{16}N_2Co_2O_8S$ (574.29): calcd. C 43.92, H 2.81, N 4.88; found C 43.69, H 2.60, N 4.50.

**[$Co_2(CO)_6$(μ-η²-$R^2CH_2CCH$)] (2):** Compound **2** was prepared using the same conditions described above for **1**, but ligand **II** was used instead to produce a deep red solid of **2** (35%) after TLC separation eluting with hexane/$CH_2Cl_2$ (1:4, v/v). IR ($CH_2Cl_2$): ν(CO) = 2098s, 2059 vs and 2033 vs $cm^{-1}$. $^1H$ NMR ($CDCl_3$): δ = 5.28 (s, 2 H, $NCH_2$), 5.75 (s, 1 H, CCH), 7.34 (t, $J_{H-H}$ = 7.3 Hz, 2 H, aromatic), 7.62 (d, $J_{H-H}$ = 7.3 Hz, 2 H, aromatic), 7.76 (t, $J_{H-H}$ = 7.3 Hz, 2 H, aromatic) and 8.59 (d, $J_{H-H}$ = 7.3 Hz, 2 H, aromatic). FAB MS: *m*/*z* = 520 [$M^+$]. $C_{22}H_{11}NCo_2O_7$ (519.20): calcd. C 50.89, H 2.14, N 2.70; found C 50.75, H 2.02, N 2.32.

**[$Fe_2(CO)_6$(μ-S*t*Bu)(μ-η²-$R^1CH_2C{=}CH_2$)] (3):** The complex [$Et_3NH$][$Fe_2(CO)_6$(μ-CO)(μ-S*t*Bu)] was freshly prepared by reacting [$Fe_3(CO)_{12}$] (101 mg, 0.20 mmol), *t*BuSH (22.5 μL, 0.20 mmol) and $NEt_3$ (27.9 μL, 0.20 mmol) in THF (15 mL) at 25−30 °C under $N_2$. This reaction mixture was then treated with **I** (57.7 mg, 0.20 mmol) and the red solution was heated to reflux for 5 h. The volatile components were removed and the residue was subjected to TLC on silica using hexane/$CH_2Cl_2$ (2:1, v/v) as eluent to afford a major deep orange product **3** in 31% yield (40.8 mg). IR ($CH_2Cl_2$): ν(N−H) = 3379 w, ν(CO) = 2070 m, 2038 vs and 1996 vs $cm^{-1}$. $^1H$ NMR ($CDCl_3$): δ = 1.35 (s, 9 H, *t*Bu), 2.63 (d, $J_{H-H}$ = 2.6 Hz, 1 H, $CCH_2$), 2.90 (s, 6 H, $NMe_2$), 3.48 (d, $J_{H-H}$ = 2.6 Hz, 1 H, $CCH_2$), 4.07 (m, 2 H, $NCH_2$), 4.83 (t, $J_{H-H}$ = 6.2 Hz, 1 H, NH), 7.21 (d, $J_{H-H}$ = 7.6 Hz, 1 H, aromatic), 7.49−7.61 (m, 2 H, aromatic), 8.25−8.33 (m, 2 H, aromatic) and 8.55 (d, $J_{H-H}$ = 8.4 Hz, 1 H, aromatic). FAB MS: *m*/*z* = 658 [$M^+$]. $C_{25}H_{26}N_2Fe_2O_8S_2$ (658.30): calcd. C 45.61, H 3.98, N 4.26; found C 45.29, H 3.67, N 4.01.

**[$Fe_2(CO)_6$(μ-S*t*Bu)(μ-η²-$R^2CH_2C{=}CH_2$)] (4):** A procedure similar to that for **3** was employed using **II** (46.7 mg, 0.20 mmol) to produce orange **4** in 35% yield (42.2 mg) following TLC purification on silica with hexane/$CH_2Cl_2$ (1:1, v/v) as eluent. IR ($CH_2Cl_2$): ν(CO) = 2068 m, 2037 vs and 1995 vs $cm^{-1}$. $^1H$ NMR ($CDCl_3$): δ = 1.41 (s, 9 H, *t*Bu), 2.77 (d, $J_{H-H}$ = 4.6 Hz, 1 H, $CCH_2$), 3.13 (d, $J_{H-H}$ = 4.6 Hz, 1 H, $CCH_2$), 5.01 (s, 2 H, $NCH_2$), 7.31 (t, $J_{H-H}$ = 7.6 Hz, 2 H, aromatic), 7.58 (d, $J_{H-H}$ = 7.6 Hz, 2 H, aromatic), 7.76 (t, $J_{H-H}$ = 7.6 Hz, 2 H, aromatic) and 8.55 (d, $J_{H-H}$ = 7.6 Hz, 2 H, aromatic). FAB MS: *m*/*z* = 603 [$M^+$]. $C_{26}H_{21}NFe_2O_7S$ (603.21): calcd. C 51.77, H 3.51, N 2.32; found C 51.49, H 3.36, N 2.18.

**[$Ru_3(CO)_9$(μ-CO)(μ₃-η²-$R^1CH_2CCH$)] (5):** To an orange solution of [$Ru_3(CO)_{10}(NCMe)_2$] prepared in situ from a mixture of [$Ru_3(CO)_{12}$] (51.1 mg, 0.08 mmol) and $NMe_3O$ (12.0 mg, 0.16 mmol) in $CH_2Cl_2$/MeCN, **I** (23.1 mg, 0.08 mmol) was added. The resulting mixture was allowed to stir at room temperature for 2 h, after which the solution was concentrated and subjected to TLC separation with pure $CH_2Cl_2$ as eluent. The title complex was isolated as a deep yellow product in 23% yield (16.0 mg). IR ($CH_2Cl_2$): ν(N−H) = 3379 w, ν(CO) = 2100 w, 2063 sh, 2055 vs, 2031s, 2012 sh and 1880 w $cm^{-1}$. $^1H$ NMR ($CDCl_3$): δ = 2.89 (s, 6 H, $NMe_2$), 3.71 (d, $J_{H-H}$ = 6.4 Hz, 2 H, $NCH_2$), 4.74 (t, $J_{H-H}$ = 6.4 Hz, 1 H, NH), 7.20 (d, $J_{H-H}$ = 7.2 Hz, 1 H, aromatic), 7.51−7.59 (m, 2 H, aromatic), 8.02 (s, 1 H, CCH), 8.20−8.23 (m, 2 H, aromatic) and 8.56 (d, $J_{H-H}$ = 8.8 Hz, 1 H, aromatic). FAB MS: *m*/*z* = 871 [$M^+$]. $C_{25}H_{16}N_2O_{12}Ru_3S$ (871.68): calcd. C 34.45, H 1.85, N 3.21; found C 34.59, H 1.90, N 3.20.

**[$Ru_3(CO)_9$(μ-CO)(μ₃-η²-$R^2CH_2CCH$)] (6):** Similar to **5**, complex **6** was synthesized from **II** (18.7 mg, 0.08 mmol) and isolated as a deep yellow solid in 27% yield (17.6 mg). IR ($CH_2Cl_2$): ν(CO) = 2101 w, 2066 vs, 2055 vs, 2034s, 2012 sh and 1881 w $cm^{-1}$. $^1H$ NMR ($CDCl_3$): δ = 5.32 (s, 2 H, $NCH_2$), 7.29−7.39 (m, 4 H, aromatic), 7.67 (s, 1 H, CCH), 7.74 (t, $J_{H-H}$ = 7.4 Hz, 2 H, aromatic) and 8.60 (dd, $J_{H-H}$ = 7.4, 1.2 Hz, 2 H, aromatic). FAB MS: *m*/*z* = 816 [$M^+$]. $C_{26}H_{11}NO_{11}Ru_3$ (816.58): calcd. C 38.24, H 1.36, N 1.72; found C 38.05, H 1.13, N 1.50.

**[$Os_3(CO)_9$(μ-CO)(μ₃-η²-$R^1CH_2CCH$)] (7):** Ligand **I** (11.5 mg, 0.04 mmol) was added to a yellow solution of [$Os_3(CO)_{10}(NCMe)_2$] (37.3 mg, 0.04 mmol) in $CH_2Cl_2$ (15 mL). The reaction mixture turned orange and stirring was continued at room temperature for 2 h. Upon removal of solvent, the residue was purified by TLC on silica using pure $CH_2Cl_2$ as eluent to give a yellow-orange product

Table 6. Summary of crystallographic data ($R1 = \Sigma||F_o| - |F_c||/\Sigma|F_o|$, $wR2 = [\Sigma w(|F_o^2| - |F_c^2|)^2/\Sigma w|F_o^2|^2]^{1/2}$)

| | 1 | 2 | 4 | 8 |
|---|---|---|---|---|
| Empirical formula | $C_{21}H_{16}N_2Co_2O_8S$ | $C_{22}H_{11}NCo_2O_7$ | $C_{26}H_{21}NFe_2O_7S$ | $C_{26}H_{11}NO_{11}Os_3$ |
| Formula mass | 574.28 | 519.18 | 603.20 | 1083.96 |
| Crystal system | Monoclinic | Triclinic | Triclinic | Monoclinic |
| Space group | $P2_1/n$ | $P\bar{1}$ | $P\bar{1}$ | $P2_1/n$ |
| *a* [Å] | 13.741(2) | 8.0188(8) | 8.778(3) | 9.4492(6) |
| *b* [Å] | 7.158(1) | 10.677(1) | 9.369(4) | 29.994(2) |
| *c* [Å] | 26.660(4) | 12.621(1) | 16.362(6) | 9.4818(6) |
| α [°] | | 88.141(2) | 100.363(6) | |
| β [°] | 90.563(3) | 83.551(2) | 96.295(7) | 92.771(1) |
| γ [°] | | 76.218(2) | 98.823(7) | |
| *V* [Å³] | 2622.1(8) | 1042.8(2) | 1294.8(9) | 2684.2(3) |
| Z | 4 | 2 | 2 | 4 |
| *T* [K] | 293 | 293 | 293 | 293 |
| *F*(000) | 1160 | 520 | 616 | 1960 |
| μ(Mo-$K_\alpha$) [$mm^{-1}$] | 1.389 | 1.635 | 1.247 | 14.229 |
| Reflections collected | 14783 | 6037 | 6499 | 15570 |
| Unique reflections | 5902 | 4403 | 4487 | 6021 |
| $R_{int}$ | 0.0618 | 0.0109 | 0.0518 | 0.0477 |
| Observed reflections | 5902 | 4403 | 4487 | 6021 |
| GOF on $F^2$ | 1.036 | 1.031 | 0.805 | 0.986 |
| *R*1, *wR*2 [$I > 2.0\sigma(I)$] | 0.0572, 0.1770 | 0.0299, 0.0837 | 0.0698, 0.1556 | 0.0328, 0.0865 |

in a moderate yield (13.7 mg, 30%). IR ($CH_2Cl_2$): ν(N−H) = 3383 w, ν(CO) = 2103 w, 2065 vs, 2054 sh, 2025s, 2006 sh and 1848 w $cm^{-1}$. $^1H$ NMR ($CDCl_3$): δ = 2.89 (s, 6 H, $NMe_2$), 3.55 (m, 1 H, $NCH_2$), 3.69 (m, 1 H, $NCH_2$), 4.64 (t, $J_{H-H}$ = 6.8 Hz, 1 H, NH), 7.19 (d, $J_{H-H}$ = 7.0 Hz, 1 H, aromatic), 7.49−7.60 (m, 2 H, aromatic), 8.16−8.21 (m, 2 H, aromatic), 8.55 (d, $J_{H-H}$ = 8.6 Hz, 1 H, aromatic) and 9.10 (s, 1 H, CCH). FAB MS: *m/z* = 1139 [$M^+$]. $C_{25}H_{16}N_2O_{12}Os_3S$ (1139.07): calcd. C 26.36, H 1.42, N 2.46; found C 26.10, H 1.20, N 2.18.

**[$Os_3(CO)_9(\mu$-CO)($\mu_3$-$\eta^2$-$R^2CH_2CCH$)] (8):** Instead of using **I**, the reaction between [$Os_3(CO)_{10}(NCMe)_2$] (37.3 mg, 0.04 mmol) and **II** (9.30 mg, 0.04 mmol) in $CH_2Cl_2$ resulted in the formation of the desired compound as a yellow solid. Purification was accomplished by TLC on silica using hexane/$CH_2Cl_2$ (1:1, v/v) as eluent to afford an analytically pure sample of **8** in 39% yield (16.9 mg). IR ($CH_2Cl_2$): ν(CO) = 2104 w, 2067 vs, 2054 vs, 2029 s, 2005 s and 1848 w $cm^{-1}$. $^1H$ NMR ($CDCl_3$): δ = 5.00 (m, 1 H, $NCH_2$), 5.19 (m, 1 H, $NCH_2$), 7.26−7.36 (m, 4 H, aromatic), 7.74 (t, $J_{H-H}$ = 7.8 Hz, 2 H, aromatic), 8.59 (dd, $J_{H-H}$ = 7.8, 1.7 Hz, 2 H, aromatic) and 8.99 (s, 1 H, CCH). FAB MS: *m/z* = 1084 [$M^+$]. $C_{26}H_{11}NO_{11}Os_3$ (1083.97): calcd. C 28.81, H 1.02, N 1.29; found C 28.90, H 1.15, N 1.43.

**X-ray Crystallography:** Good-quality crystals of our compounds suitable for X-ray diffraction studies were grown by slow evaporation of their respective solutions in hexane−$CH_2Cl_2$ at room temperature. Geometric and intensity data were collected using graphite-monochromated Mo-$K_\alpha$ radiation (λ = 0.71073 Å) on a Bruker AXS SMART 1000 CCD area-detector diffractometer. The collected frames were processed with proprietary software SAINT[47] and an absorption correction was applied (SADABS[48]) to the collected reflections. The structures of these molecules were solved by direct methods and expanded by standard difference Fourier syntheses using the software SHELXTL.[49] Structure refinements were made on $F^2$ by the full-matrix least-squares technique. All other non-hydrogen atoms were refined with anisotropic displacement parameters. Hydrogen atoms were either generated from Fourier maps or placed in their idealized positions and allowed to ride on the respective carbon atoms. Pertinent crystallographic information is provided in Table 6.

CCDC-174709 to -174712 contain the supplementary crystallographic data for this paper. These data can be obtained free of charge at www.ccdc.cam.ac.uk/conts/retrieving.html [or from the Cambridge Crystallographic Data Centre, 12, Union Road, Cambridge CB2 1EZ, UK; Fax: (internat.) +44−1223/336−033; E-mail: deposit@ccdc.cam.ac.uk].

## Acknowledgments

W.-Y.W. thanks the Hong Kong Research Grants Council (HKBU 2022/99P) and the Hong Kong Baptist University for financial support.

[1] A. Mayer, S. Neuenhofer, *Angew. Chem. Int. Ed. Engl.* **1994**, *33*, 1044−1072.
[2] A. P. de Silva, H. Q. N. Gunaratne, T. Gunnlaugsson, A. J. M. Huxley, C. P. McCoy, J. T. Rademacher, T. E. Rice, *Chem. Rev.* **1997**, *97*, 1515−1566, and references therein.
[3] L. Fabbrizzi, A. Poggi, *Chem. Soc. Rev.* **1995**, 197−202, and references therein.
[4] A. P. de Silva, H. Q. N. Gunarantne, T. Gunnlaugsson, A. J. M. Huxley, C. P. McCoy, J. T. Rademacher, T. E. Rice, *Advances in Supramolecular Chemistry,* vol. 4, Jai Press Inc., **1997**, p. 1−53.
[5] *Fluorescent Chemosensors for Ion and Molecular Recognition* (Ed.: A. W. Czarnik), American Chemical Society, Washington, DC, **1992**.
[6] L. Fabbrizzi, M. Licchelli, P. Pallavicini, L. Parodi, A. Taglietti, *Transition Metals in Supramolecular Chemistry* (Ed.: J. P. Sauvage), Wiley, **1999**, p. 93−135.
[7] F. Bolletta, D. Fabbri, M. Lombardo, L. Prodi, C. Trombini, N. Zaccheroni, *Organometallics* **1996**, *15*, 2415−2417.
[8] L. Prodi, F. Bolletta, M. Montalti, N. Zaccheroni, *Eur. J. Inorg. Chem.* **1999**, 455−460.
[9] W.-Y. Wong, K.-Y. Tsang, K.-H. Tam, G.-L. Lu, C. Sun, *J. Organomet. Chem.* **2000**, *601*, 237−245.
[10] W.-Y. Wong, K.-H. Choi, K.-W. Cheah, *J. Chem. Soc., Dalton Trans.* **2000**, 113−115.
[11] J. Lewis, N. J. Long, P. R. Raithby, G. P. Shields, W.-Y. Wong, M. Younus, *J. Chem. Soc., Dalton Trans.* **1997**, 4283−4288.
[12] J. Lewis, P. R. Raithby, W.-Y. Wong, *J. Organomet. Chem.* **1998**, *556*, 219−228.
[13] N. Chawdhury, A. Köhler, R. H. Friend, W.-Y. Wong, J. Lewis, M. Younus, P. R. Raithby, T. C. Corcoran, M. R. A. Al-Mandhary, M. S. Khan, *J. Chem. Phys.* **1999**, *110*, 4963−4970.
[14] W.-Y. Wong, W.-K. Wong, P. R. Raithby, *J. Chem. Soc., Dalton Trans.* **1998**, 2761−2766.
[15] W.-Y. Wong, S.-M. Chan, K.-H. Choi, K.-W. Cheah, W.-K. Chan, *Macromol. Rapid Commun.* **2000**, *21*, 453−457.
[16] W.-Y. Wong, K.-H. Choi, G.-L. Lu, J.-X. Shi, *Macromol. Rapid Commun.* **2001**, *22*, 461−465.
[17] S. L. Murov, I. Carmichael, G. L. Hug, *Handbook of Photochemistry* Dekker, New York, **1993**.
[18] D. Seyferth, J. B. Hoke, G. B. Womack, *Organometallics* **1990**, *9*, 2662−2672.
[19] J. Suades, R. Mathieu, *J. Organomet. Chem.* **1986**, *312*, 335−341.
[20] P. R. Raithby, M. J. Rosales, *Adv. Inorg. Chem. Radiochem.* **1985**, *29*, 169−247.
[21] L. P. Clarke, J. E. Davies, P. R. Raithby, G. P. Shields, *J. Chem. Soc., Dalton Trans.* **1996**, 4147−4148.
[22] L. P. Clarke, *Ph.D. Thesis,* University of Cambridge, **1997**.
[23] C. J. Adams, L. P. Clarke, A. M. Martin-Castro, P. R. Raithby, G. P. Shields, *J. Chem. Soc., Dalton Trans.* **2000**, 4015−4017.
[24] A. J. Deeming, A. M. Senior, *J. Organomet. Chem.* **1992**, *439*, 177−188.
[25] C. E. Housecroft, B. F. G. Johnson, M. S. Khan, J. Lewis, P. R. Raithby, M. E. Robson, D. A. Wilkinson, *J. Chem. Soc., Dalton Trans.* **1992**, 3171−3178.
[26] S. M. Draper, M. Delamesiere, E. Champeil, B. Twamley, J. J. Byrne, C. Long, *J. Organomet. Chem.* **1999**, *589*, 157−167.
[27] X. Verdaguer, A. Moyano, M. A. Pericàs, A. Riera, A. Alvarez-Larena, J.-F. Piniella, *Organometallics* **1999**, *18*, 4275−4285.
[28] W.-Y. Wong, H.-Y. Lam, S.-M. Lee, *J. Organomet. Chem.* **2000**, *595*, 70−80.
[29] D. Seyferth, J. B. Hoke, J. C. Dewan, *Organometallics* **1994**, *13*, 3452−3464.
[30] L. F. Dahl, C.-H. Wei, *Inorg. Chem.* **1963**, *2*, 328−333.
[31] D. Seyferth, G. B. Womack, J. C. Dewan, *Organometallics* **1985**, *4*, 398−400.
[32] *International Tables for X-ray Crystallography*, (Eds.: C. M. MacGillavry, G. D. Rieck), Kynoch Press, Birmingham, England, **1974**, vol. 3, p. 276.
[33] G. Schaftenaar, Molden, version 3.5, CAOS/CAMM Center Nijmegen, Toernooiveld, Nijmegen, The Netherlands, **1999**.
[34] M. J. Calhorda, E. Hunstock, L. F. Veiros, F. Hartl, *Eur. J. Inorg. Chem.* **2001**, 223−231.
[35] J. Nijhoff, F. Hartl, J. W. M. van Outersterp, D. J. Stufkens, M. J. Calhorda, L. F. Veiros, *J. Organomet. Chem.* **1999**, *573*, 121−133.
[36] J. N. Nicholls, M. D. Vargas, *Inorg. Synth.* **1990**, *28*, 292−293.
[37] A. J. Blake, P. J. Dyson, B. F. G. Johnson, C. M. Martin, J. G.

M. Nairn, E. Parisini, J. Lewis, *J. Chem. Soc., Dalton Trans.* **1993**, 981−984.
[38] W. R. Dawson, M. W. Windsor, *J. Phys. Chem.* **1968**, *72*, 3251−3260.
[39] A. D. Decke, *J. Chem. Phys.* **1993**, *98*, 5648−5652.
[40] B. Miehlich, A. Savin, H. Stoll, H. Preuss, *Chem. Phys. Lett.* **1989**, *157*, 200−206.
[41] C. Lee, W. Yang, G. Parr, *Phys. Rev. B* **1988**, *37*, 785−789.
[42] P. C. Hariharan, J. A. Pople, *Theor. Chim. Acta* **1973**, *28*, 213−222.
[43] P. J. Hay, W. R. Wadt, *J. Chem. Phys.* **1985**, *82*, 299−310.
[44] M. J. Frisch, G. W. Trucks, H. B. Schlegel, G. E. Scuseria, M. A. Robb, J. R. Cheeseman, V. G. Zakrzewski, J. A. Montgomery Jr., R. E. Stratmann, J. C. Burant, S. Dapprich, J. M. Millam, A. D. Daniels, K. N. Kudin, M. C. Strain, O. Farkas, J. Tomasi, V. Barone, M. Cossi, R. Cammi, B. Mennucci, C. Pomelli, C. Adamo, S. Clifford, J. Ochterski, G. A. Petersson, P. Y. Ayala, Q. Cui, K. Morokuma, D. K. Malick, A. D. Rabuck, K. Raghavachari, J. B. Foresman, J. Cioslowski, J. V. Ortiz, B. B. Stefanov, G. Liu, A. Liashenko, P. Piskorz, I. Komaromi, R. Gomperts, R. L. Martin, D. J. Fox, T. Keith, M. A. Al-Laham, C. Y. Peng, A. Nanayakkara, C. Gonzalez, M. Challacombe, P. M. W. Gill, B. Johnson, W. Chen, M. W. Wong, J. L. Andres, C. Gonzalez, M. Head-Gordon, E. S. Replogle, J. A. Pople, *Gaussian 98* (Revision A.5); Gaussian, Inc.: Pittsburgh (PA), **1998**.
[45] W.-Y. Wong, G.-L. Lu, K.-F. Ng, K.-H. Choi, Z. Lin, *J. Chem. Soc., Dalton Trans.* **2001**, 3250−3260.
[46] W.-Y. Wong, K.-H. Choi, G.-L. Lu, J.-X. Shi, P.-Y. Lai, S.-M. Chan, Z. Lin, *Organometallics* **2001**, *20*, 5446−5454.
[47] *SAINT, Reference manual*, Siemens Energy and Automation, Madison, WI, **1994**−**1996**.
[48] G. M. Sheldrick, SADABS, Empirical Absorption Correction Program, University of Göttingen, Germany, **1997**.
[49] G. M. Sheldrick, *SHELXTL*™, *Reference manual*, version 5.1, Siemens, Madison, WI, **1997**.

Received December 5, 2001
[I01499]